DOI: 10.1534/genetics.109.107540

Identification of Novel Genes That Mediate Innate Immunity Using Inbred Mice

Ivana V. Yang,*,†,[1] Claire M. Wade,‡,§ Hyun Min Kang, Scott Alper,†,†† Holly Rutledge,‡‡ Brad Lackford,‡‡ Eleazar Eskin,§§ Mark J. Daly‡,§ and David A. Schwartz*,†**

*Department of Medicine, †Center for Genes, Environment, and Health, and ††Department of Immunology, National Jewish Health, Denver, Colorado 80206, ‡Center for Human Genetic Research, Massachusetts General Hospital, Boston, Massachusetts 02114, §Broad Institute of Harvard University and Massachusetts Institute of Technology, Cambridge, Massachusetts 02142, **Department of Computer Science and Engineering, University of California, San Diego, La Jolla, California 92093, ‡‡National Institute of Environmental Health Sciences, Research Triangle Park, North Carolina 27709 and §§Department of Computer Science and Department of Human Genetics, University of California, Los Angeles, California 90095

Manuscript received July 20, 2009
Accepted for publication September 23, 2009

ABSTRACT

Innate immunity is the first line of defense against microbial infections. Although polymorphisms in toll-like receptors (TLRs) and downstream signaling molecules (CD14, TLR2, TLR4, TLR5, and IRAK4) affect the innate immune response, these variants account for only a portion of the ability of the host to respond to bacteria, fungi, and viruses. To identify other genes involved in the innate immune response, we challenged 16 inbred murine strains with lipopolysaccharide (LPS) systemically and measured serum concentrations of pro-inflammatory cytokines IL-1β, IL-6, and TNFα, and the chemokine KC 6 hr post-treatment. Loci that segregate with strain phenotypes were identified by whole genome association (WGA) mapping of cytokine concentrations. Published gene expression profiles and quantitative trait loci (QTL) were then utilized to prioritize loci and genes that potentially regulate the host response to LPS. Sixteen loci were selected for further investigation by combining WGA analysis with previously published QTL for murine response to LPS or gram negative bacteria. Thirty-eight genes within these loci were then selected for further investigation on the basis of the significance of the identified locus, transcriptional response to LPS, and biological plausibility. RNA interference-mediated inhibition of 4 of 38 candidate genes was shown to block the production of IL-6 in J774A.1 macrophages. In summary, our analysis identified 4 genes that have not previously been implicated in innate immunity, namely, 1110058L19Rik, 4933415F23Rik, Fbxo9, and Ipo7. These genes could represent potential sepsis biomarkers or therapeutic targets that should be further investigated in human populations.

LIPOPOLYSACCHARIDE (LPS), a major component of the cell wall of gram negative (GN) bacteria, is a potent stimulator of the innate immune response in mice and humans. Binding of LPS to the receptor complex consisting of TLR4, CD14, and MD-2 initiates a signaling cascade that leads to translocation of NF-κB into the nucleus and the release of pro-inflammatory cytokines and chemokines (Akira and Takeda 2004). This inflammatory response affects development and progression of a number of diseases including sepsis and septic shock. However, antiinflammatory agents have failed in the treatment of the systemic inflammatory response induced by sepsis due to the pathophysiologic complexity of the syndrome that involves cardiovascular, immunological, and endocrine systems (Baron *et al.* 2006). It is therefore imperative to develop new therapeutic targets for treating patients at risk of developing the inflammatory response to sepsis.

Genetic factors play a significant role in the regulation of systemic inflammation. In addition to representing potential therapeutic targets for diseases such as sepsis, innate immune genes could also be used to identify individuals at highest risk for complications from sepsis. Polymorphisms in genes in the TLR4 pathway (TLR4, CD14, IRAK4), downstream pro-inflammatory cytokines (TNFα, IL-1β, IL-6), as well as genes in the coagulation/fibrinolysis cascade (PAI1, Factor V, TAFI) and other pathways (MBL, heat shock proteins) have been shown to predispose individuals for increased susceptibility to sepsis and adverse outcomes (Cook *et al.* 2004a; Papathanassoglou *et al.* 2006; Garantziotis *et al.* 2008).

Many features of human disease pathophysiology are successfully recapitulated in animal models of sepsis (Buras *et al.* 2005). The systemic LPS or endotoxemia model involves a bolus injection of LPS and is

Supporting information is available online at http://www.genetics.org/cgi/content/full/genetics.109.107540/DC1.

[1]*Corresponding author:* Department of Medicine, National Jewish Health, 1400 Jackson St., A630, Denver, CO 80206.
E-mail: yangi@njhealth.org

characterized by an overwhelming innate immune response, mediated by pro-inflammatory cytokines such as TNF-α that are produced rapidly (several hours) post-LPS injection. This strong cytokine response can ultimately lead to multiple organ failure and death. Studies performed in murine models support the notion that genetic background plays a significant role in development and progression of infection. For example, there is a range of responses among inbred strains of mice to inhaled (Lorenz *et al.* 2001) and systemic LPS (De Maio *et al.* 1998).

Genetic studies in mice have been used extensively to identify novel innate immune genes that potentially contribute to host defense against microbial infections. QTLs controlling various aspects of inflammation and survival in response to LPS (Matesic *et al.* 1999, 2000; Cook *et al.* 2004b; Fulton *et al.* 2006) and different species of Salmonella (Sebastiani *et al.* 1998; Caron *et al.* 2002, 2005) have been identified using F_2 intercrosses between inbred strains of mice, recombinant inbred (RI) panels, and congenic strains. However, as is the case with mapping of other complex traits, QTL studies in mice identify large genomic regions of interest, and very rarely lead to identification of a single gene controlling differences in response in the two parent strains, even when combined with other approaches such as fine mapping and gene expression profiling.

Recent advances in genomic sequence analysis and SNP discovery have led to the availability of dense SNP maps for a large number of inbred strains of mice (Frazer *et al.* 2007). These dense mouse SNP maps are a rich resource for mapping of complex traits and have been used for both GWA mapping (Grupe *et al.* 2001; Liu *et al.* 2006; McClurg *et al.* 2007) and for refinement of previously identified QTL (Pletcher *et al.* 2004). In the present study, we measured serum concentrations of the pro-inflammatory cytokines IL-1β, IL-6, and TNFα, and the chemokine KC, following systemic administration of LPS in 16 inbred strains of mice. We subsequently performed WGA mapping to identify loci that segregate with strain cytokine/chemokine phenotypes. We prioritized the loci and genes identified by this *in silico* approach by combining the results with previously published QTL and gene expression profiles. The role of 38 candidates revealed by this combined analysis in controlling inflammatory response to LPS was tested by RNA interference in a mouse macrophage cell line. Four genes (1110058L19Rik, 4933415F23Rik, Fbxo9, and Ipo7) affected LPS-induced cytokine production in this assay and are therefore high-priority novel innate immune targets for the potential development of therapeutics and for risk profiling.

MATERIALS AND METHODS

Animal model: We used an established model of endotoxic shock in which mice are injected with a high dose of LPS with no D-galactosamine sensitization (Buras *et al.* 2005). All procedures were approved by the animal care and use committees at Duke University Medical Center, the National Institute of Environmental Health Sciences, and the National Heart, Lung, and Blood Institute. Mice were injected intraperitoneally with 125,000 EU/g body weight of *Escherichia coli* 0111:B4 LPS (Sigma) or sterile saline control.

One group of mice that received LPS ($N = 8$) was observed for clinical signs of morbidity over 5 days and euthanized according to guidelines set by Morton and Griffiths (1985). The study was repeated and combined data were used to construct Kaplan-Meier survival curves. Animals that received saline only ($N = 8$) were also observed for 5 days and exhibited no signs of morbidity. The second group of animals ($N = 8$) was euthanized 6-hr post-LPS challenge for serum and organ collection. Control mice ($N = 8$) were euthanized 6 hr following the saline injection. Serum concentrations of IL-1β, IL-6, KC, and TNFα were determined using standard ELISA kits and the manufacturer's protocol (R&D Systems).

Whole genome association mapping using Plink: Genotype files were extracted for 138,793 curated mouse haplotype map SNPs (⟨http://www.broad.mit.edu/mouse/⟩) for each of the strains used in mapping (129S1/SvImJ, A/J, AKR/J, BALB/cByJ, BUB/BnJ, C57BL/6J, CE/J, DBA/2J, FVB/NJ, LP/J, MA/MyJ, NOD/LTJ, NON/LtJ, and NZW/LacJ). The SM/J strain was excluded from this analysis because of the low genotyping rate in the database (>10% missing genotypes). The CAST/Ei strain was excluded from the analysis because the genetic differences between wild-derived and classical inbred strains are difficult to account for in mapping studies (Wade and Daly 2005). Map files corresponded to the identities and positions of these SNP on the 2004 Mouse Assembly (mm3). Log_{10}-transformed mean serum concentrations of IL-1β, IL-6, KC, and TNFα for each strain were analyzed using the genetic analysis program Plink v0.99d (Purcell *et al.* 2007) to perform quantitative association. For all analyses, SNPs with minor allele frequency (MAF) <0.1 were excluded and adaptive permutation was employed to assess significance of association. After pruning of strains and SNP, 84,253 SNP and 14 strains remained in the analysis.

Whole genome association mapping using EMMA: In addition to our analysis using the Plink software, we analyzed the murine data using a recently established method that accounts for different degrees of relatedness among inbred strains of mice (Kang *et al.* 2008). This efficient mixed model association (EMMA) algorithm was applied to log_{10}-transformed individual measurements of serum cytokine concentrations in 15 strains of mice using haplotype map SNPs. CAST/Ei strain was included in this analysis because EMMA adequately accounts for genetic diversity of wild-derived and classical inbred strains of mice.

RNA interference: RNA interference assays were carried out as recently described (Alper *et al.* 2008). Briefly, siRNAs (Dharmacon, pools of four siRNA duplexes/gene) were transfected into the mouse macrophage cell line J774A.1 using the Amaxa Nucleofector Shuttle according to the manufacturer's instructions. Transfections were carried out in 96-well format using 100,000 cells/well and 2 μM siRNA. Twenty-four to 36 hr after siRNA transfection, LPS was added to a final concentration of 20 ng/ml LPS (List Biological Labs). Supernatant was collected 5 hr post-LPS treatment, and cytokine production was assayed using the Lincoplex kit (Linco) and read on a Luminex system (Bio-Rad). Cell viability was monitored and cell number normalized using fluorescein diacetate . Cytokine production was normalized relative to a negative control siRNA. RNA was isolated using the RNAEasy kit (Qiagen) and the extent of gene knockdown was monitored by real-time RT–PCR with SYBR Green on an ABI 7900HT sequence

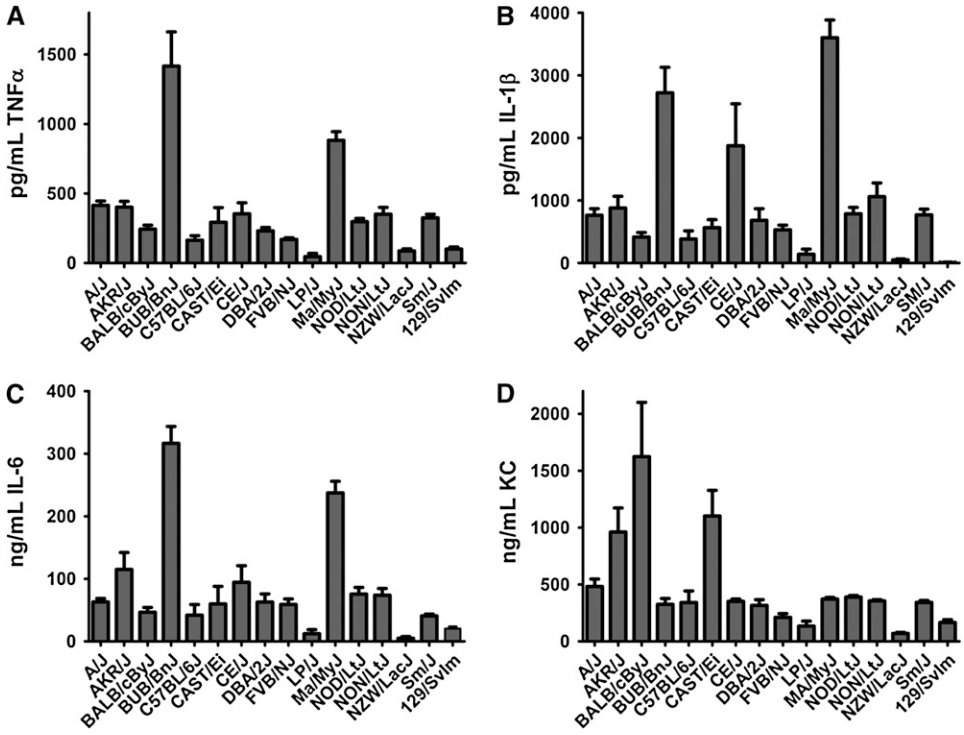

FIGURE 1.—Cytokine production by inbred strains of mice. Serum concentrations of TNFα (A), IL-1β (B), IL-6 (C), and KC (D) for 16 inbred strains 6 hr post-intraperitoneal LPS challenge. Values shown are means with SEMs for $N = 8$.

detection system (Applied Biosystems). siRNAs were initially tested in triplicate, and siRNAs that had an effect were assayed three additional times using different concentrations of siRNA (2 μM, 1 μM, 0.5 μM, and 0.25 μM). siRNAs that still affected cytokine production after these retests were further tested by transfecting each siRNA in the pool individually to verify that multiple siRNAs targeting each gene could still induce the same phenotype.

RESULTS

Inbred mouse strain phenotypes: To study the genetic basis of the inflammatory response to LPS, we challenged 16 inbred strains of mice represented in the mouse haplotype map project at the Broad Institute (WADE and DALY 2005) with LPS systemically and measured concentrations of IL-1β, IL-6, KC, and TNFα in the serum 6 hr following administration of LPS. We observed a range of phenotypes from almost no cytokine production to ng/ml range for TNFα and IL-1β, and to several hundreds to over a thousand ng/ml for IL-6 and KC (Figure 1) with both consistencies and discrepancies in the production of different cytokines/chemokine in response to LPS in the strains examined. Three strains of mice, 129/SvIm, NZW/LacJ, and LP/J, produce consistently low serum concentrations of all three cytokines and the chemokine KC. On the other hand, the MA/MyJ and BUB/BnJ strains produce very high concentrations of the pro-inflammatory cytokines IL-1β, IL-6, and TNFα but an intermediate concentration of the chemokine KC relative to other strains examined. These observations suggest that both common and diverse genetic factors contribute to production of IL-1β, IL-6, TNFα, and KC in response to systemic LPS challenge. Saline-injected control animals produced low concentrations of all inflammatory markers with very little variation among different strains of mice.

The strong inflammatory response induced by LPS in these mice can ultimately lead to organ failure and death. We therefore also monitored a separate group of the inbred mouse strains for survival over the course of 5 days following LPS injection and found that 13 of the strains studied were sensitive (>75% morbidity within 48 hr post-LPS) and 3 strains (129/SvIm, C57/BL6, and NZW/LacJ) were resistant to LPS (<25% morbidity at the end of 5 days) (supporting information, Figure S1). Two out of three resistant strains (129/SvIm and NZW/LacJ) have low serum concentrations of IL-1β, IL-6, KC, and TNFα following LPS challenge, which is consistent with the idea that the extent of inflammatory cytokine production affects LPS-induced mortality. However, some of the sensitive strains, especially LP/J, also produce low amounts of the cytokines measured, indicating that factors other than pro-inflammatory cytokines in the serum also contribute to mortality following LPS challenge.

Whole genome association mapping: To identify loci that segregate with inflammatory phenotypes (IL-1β, IL-6, TNFα, and KC production) in inbred strains, we performed whole genome association mapping by analyzing HapMap SNP data using two different statistical approaches. In one approach, we mapped cytokine/chemokine concentrations as quantitative traits by standard linear regression of phenotype on allele dosage as implemented in the Plink software (PURCELL

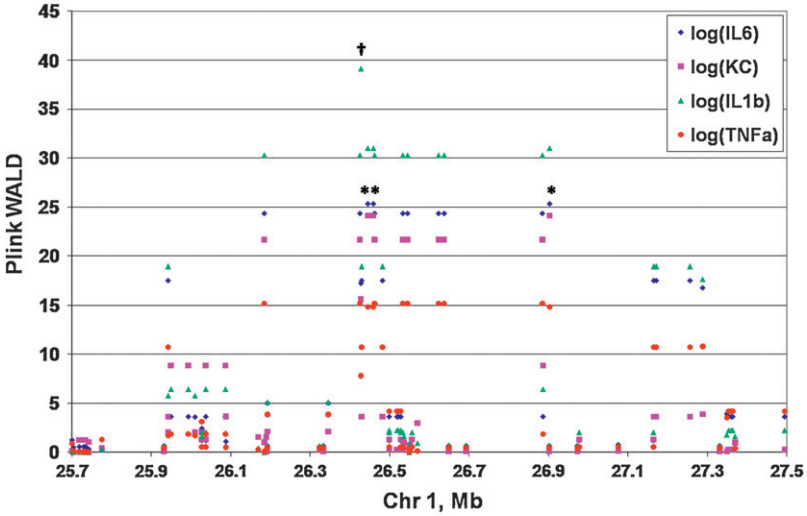

FIGURE 2.—Whole genome association mapping. Plink Wald statistic values for SNPs in each of the loci were plotted to identify the extent of linkage disequilibrium (LD) and determine the boundaries of each locus. Shown is the graph for locus 1 on chromosome 1. *, three SNPs most highly associated ($P = 4.9 \times 10^{-7}$) with IL-6 concentrations; †, the most associated SNP ($P = 3.9 \times 10^{-10}$) with IL-1β production.

et al. 2007). A number of SNPs with $P < 1 \times 10^{-5}$ were associated with each of the four cytokine production phenotypes, for a total of 38 unique loci, with some of the identified loci regulating the production of several cytokines/chemokine (Table S1 and Figure S2 A). To determine the boundaries of each of the statistically significant loci, we plotted Wald statistic values for the top associated ($P < 1 \times 10^{-5}$) and neighboring SNPs for each locus identified; an example of this analysis is depicted in Figure 2 for a representative locus on chromosome 1.

In another approach, we utilized a statistical method that was recently developed specifically for association mapping in model organisms called efficient mixed model association (EMMA) (KANG *et al.* 2008). In this method, a linear mixed model is incorporated into the analysis to correct for population structure and genetic relatedness among inbred strains of mice. EMMA analysis also identified a number of SNPs throughout the genome that segregate with the strain cytokine phenotypes ($P < 0.001$), but the number of associated SNPs/locus is fewer than in the Plink analysis (27 unique loci) (Table S2 and Figure S2 B). Five out of 27 loci identified by EMMA were also identified by Plink, suggesting only a modest degree of overlap and providing justification for using both methods.

Candidate loci and gene selection for further investigation: To prioritize loci for further investigation, we considered four factors: whether the locus lies within a previously published QTL for response to LPS or a GN pathogen, whether the locus was identified as significant by both statistical methods, whether the locus was identified as regulating the production of more than one cytokine/chemokine, and the level of statistical significance in one or both of the whole genome association analyses. Sixteen loci met at least one of the four criteria (Table 1). The majority of these loci are 1.5–4.5 Mb in size with two exceptions, locus number 8 on chromosome 7 and the locus on chromosome 13, where linkage disequilibrium extends over 23.5 and 10 Mb, respectively. There are 676 known genes within these 16 loci, with some loci being much more gene rich than others (two loci contain no known genes) (Table S3). It is likely that several of these 676 genes could represent novel innate immune regulators.

To identify a reasonable number of high-priority candidates, out of 676 identified, to screen in a medium-throughput RNAi assay in mouse macrophages (ALPER *et al.* 2008), we used three approaches. We first selected all 11 genes in the three loci identified by both whole genome association analyses (Plink and EMMA) that also lie within published QTL (Figure 3A; loci nos. 1, 2, and 6 in Table 1). Second, we overlaid the results from our unpublished gene expression data set (I. YANG and D. SCHWARTZ, unpublished results) from 11 inbred strains of mice, the majority of which are included in the current study, on all 16 loci. By combining mapping data from this work with transcriptional response data from our unpublished data, we identified 62 candidates as differentially expressed genes (in at least one organ) within one of the 16 loci of interest (Figure 3B and Table 2). Thus, using the first two approaches, we identified 72 gene candidates for further study (11 from the first approach, 62 from this second approach; 1 of the 11 genes in the three loci identified above, 1110058L19RIK, is also differentially expressed). Finally, we then chose 38 of these 72 candidates for further functional investigation on the basis of their predicted function. We included genes that have a known role in immunity (Itgam, for example), those that could have a potential role (kinases, proteases, transcription factors), and genes of unknown function. We excluded genes involved in metabolism, those encoding ribosomal proteins, methyltransferases, and a few others.

RNA interference of 38 candidate genes identifies four novel innate immune genes: To test the role of the selected candidate genes in innate immunity, we transfected the J774A.1 mouse macrophage cell line with

TABLE 1

Sixteen *in silico* loci chosen as high priority loci controlling serum cytokine concentrations in inbred murine strains in response to systemic LPS challenge

Locus no.	Chr	Locus boundaries (Mb)	Phenotype	Method	Associated SNP (Mb)	*P*-value(s)	Published QTL
1	1	23–28	IL-1β	Plink	26427831	3.90*E*-10	**1**
			IL-6	Plink	26445071, 26459079, 26902686	4.90*E*-07	
			KC	EMMA	24076131, 24330584, 24967418, 24967436, 26414682	5.6*E*-3; 6.8*E*-3	
2	1	145.5–147	KC	Plink	145683060	1.20*E*-07	**2**
			TNFα	EMMA	14672597	6.40*E*-03	
3	2	68–70	KC	Plink	69438537	1.20*E*-07	**3**
4	2	80.5–82.5	KC	Plink	80841547, 80883004, 81138233, 81560669, 81615533, 81617733, 81628234, 81658448, 81659050, 81678285, 81704287, 81718343, 81789194, 82079297, 82079512, 82084458, 82117829, 82122611, 82126777, 82143108, 82143635	1.20*E*-07	**3**
5	2	106.5–109	IL-1 β	EMMA	107315924, 107357384, 107398624, 107412136, 107959779, 108073860, 108185629	5.40*E*-03	**3**
6	5	78–82	IL-6	Plink	79316768, 79549852, 80265545	4.90*E*-07	**4**
			KC	EMMA	80712378, 81426649	6.80*E*-03	
7	6	59.5–64	TNFα	Plink	61560974	5.20*E*-06	
			IL-6	Plink	61560974	4.40*E*-08	
			KC	EMMA	62063800, 61240554	6.9*E*-3; 7.1*E*-3	
8	7	82.5–106	TNFα	Plink	8853602, 9333316	5.20*E*-06	**5**
			IL-6	Plink	8853602, 9333316	4.40*E*-08	
			IL-1β	Plink	9595330	3.90*E*-10	
9	7	115–118	IL-1β	Plink	116601809	3.90*E*-10	**5**
			IL-6	Plink	116916407	4.90*E*-07	
10	8	21–23.5	IL-6	EMMA	22106945, 22224999, 22185337, 22262697, 22277352, 22115030	8*E*-4; 1.2*E*-3; 1.3*E*-3; 1.5*E*-3; 1.4*E*-3	
			KC	Plink	22416276, 22536836	1.20*E*-07	
11	9	78–81.5	TNFα	Plink	79331943, 80661899	5.2*E*-6; 9.1*E*-6	
			IL-1β	Plink	80149240	3.90*E*-10	
			IL-6	Plink	80661899	4.40*E*-08	
12	11	56.2–60.2	IL-6	EMMA	59250160	8.00*E*-04	**6–8**
			KC	EMMA	57287378	5.60*E*-03	
13	13	48–58	IL-6	EMMA	5173293, 5273676, 5461529, 5675544,	1.40*E*-03	**9, 10**
14	14	27–30	IL-1β	Plink	28372705	3.90*E*-10	
			IL-6	Plink	28800101	4.90*E*-07	
15	14	91.3–93	IL-1β	Plink	91942359, 92310781	3.90*E*-10	
			KC	Plink	92145464	1.20*E*-07	
16	15	31.5–33	TNFα	Plink	32506173	5.20*E*-06	**11, 12**
			IL-1β	Plink	32541454	3.90*E*-10	
			IL-6	Plink	32504050, 32506173	4.9*E*-7; 4.4*E*-8	

1, Ses1.1 locus; bacterial load in the spleen in response to iv S. enteritidis in (C57BL/6J × 129S6) F2 intercross and 129.B6-Ses1.1 congenic mice (Caron *et al.* 2002, 2005); **2**, Susceptibility to iv *S. typhimurium* in (C57BL/6J × MOLF/Ei) F_2 mice (Sebastiani *et al.* 1998); **3**, Lptl1 locus; pulmonary TNFα levels following aerosolized LPS challenge in (C57BL/6J × DBA/2J) F_2 and RI mice (Cook *et al.* 2004b); **4**, Hpi2 locus; hepatic PMN infiltration in response to systemic LPS in BXA RI mice (Matesic *et al.* 2000); **5**, Ses2 locus; bacterial load in the spleen in response to iv *S. enteritidis* in (C57BL/6J × 129S6) F_2 intercross and 129.B6-Ses2 congenic mice (Caron *et al.* 2002, 2005); **6**, Lppl1 and Lptl2 loci; pulmonary PMN recruitment and TNFα levels following aerosolized LPS challenge in (C57BL/6J × DBA/2J) F_2 and RI mice (Cook *et al.* 2004b); **7**, Mol4 locus; splenocyte proliferation *in vitro* following systemic LPS challenge in AXB and BXA RI strains (Matesic *et al.* 1999); **8**, Susceptibility to iv *S. typhimurium* in (C57BL/6J × MOLF/Ei) F_2 mice (Sebastiani *et al.* 1998); **9**, Hpi1 locus; hepatic PMN infiltration in response to systemic LPS in BXA RI mice (Matesic *et al.* 2000); **10**, Mol3 locus; splenocyte proliferation *in vitro* following systemic LPS challenge in AXB and BXA RI strains (Matesic *et al.* 1999); **11**, Ses3 locus; bacterial load in the spleen in response to iv *S. enteritidis* in (C57BL/6J × 129S6) F_2 intercross and 129.B6-Ses3 congenic mice (Caron *et al.* 2002, 2005); **12**, Susceptibility to iv *S. typhimurium* in (C57BL/6J × MOLF/Ei) F_2 mice (Sebastiani *et al.* 1998).

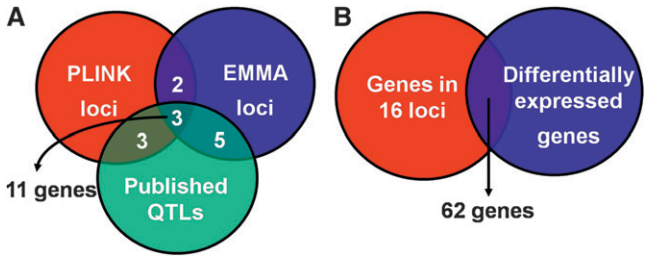

Figure 3.—Strategy used to prioritize genes for further investigation. (A) Identification of three loci containing 11 genes. These three loci were mapped by both Plink and EMMA methods and overlap with published QTLs. (B) Sixty-two genes within all 16 loci are differentially expressed in at least one organ (liver, lung, and spleen) of strains sensitive to LPS challenge compared to resistant strains in response to systemic LPS challenge (I. Yang and D. Schwartz, unpublished results). By combining the two approaches (overlap of all three mapping approaches in Figure 3A and overlap of at least one mapping approach with expression profiling in Figure 3B), 72 candidate genes were identified (1 gene, 1110058L19RIK, was common to both approaches).

siRNA pools (made up of four siRNA duplexes per gene) for the 38 candidate genes, stimulated the cells with LPS, and measured cytokine production. Pooling of four siRNA duplexes greatly reduces off-target effects of individual siRNAs, while maintaining high levels of target silencing (Svoboda 2007). Shown in Figure 4A are the results of this initial RNAi screen for inhibition of IL-6 production for the 38 candidates. As expected, several negative control siRNA treatments that do not target any gene had little or no effect on cytokine production (first four siRNA treatments in Figure 4A). Inhibition of genes known to be involved in the response to LPS, including the LPS receptor TLR4, the signaling adaptor CD14, and IL-6 itself, strongly blocked the production of IL-6, serving as positive controls for the assay (Figure 4A). In addition, RNAi-mediated inhibition of 12 of the 38 candidate genes prevented the production of IL-6 by ≥50%. On the basis of this initial screen, we repeated the assay three additional times for these 12 candidates using decreasing concentrations of siRNA (2 μM, 1 μM, 0.5 μM, and 0.25 μM). These data showed that knockdown of four genes (1110058L19Rik, 4933415F23Rik, Fbxo9, and Ipo7) consistently inhibited production of IL-6, with the effect lost at lower siRNA concentrations (Figure 4B). We also measured the extent of RNA knockdown in this titration data set using real time RT–PCR and showed that the siRNA-mediated inhibition of IL-6 production correlates with RNAi knockdown (Figure 4C). To verify that the siRNA effect was specific, we transfected each of the four individual siRNAs in the pool into macrophages, and found that at least two out of the four individual siRNAs in each pool significantly inhibit production of IL-6 (Figure 4D), demonstrating that multiple siRNAs targeting each gene can induce the same phenotype. Taken together, the data in Figure 4 demonstrate that knockdown of four candidate innate immune genes inhibits cytokine production and that these data are not false positives due to off-target effects of RNA interference.

DISCUSSION

By integrating WGA mapping of cytokine/chemokine phenotypes in inbred mouse strains with additional genetic and genomic studies, we have identified four novel genes that regulate the inflammatory response to LPS. We utilized two related but somewhat divergent statistical approaches to determine polymorphisms throughout the mouse genome that are most significantly associated with serum concentrations of IL-1β, IL-6, KC, and TNFα. More loci with lower *P*-values were identified using the Plink method than EMMA due to the fact that Plink does not account for the population structure in the inbred mouse strains. Because of this, some of the significant loci identified by Plink but not EMMA may be false positives. However, only a modest degree of overlap in loci identified by Plink and EMMA justifies the use of both methods. Since mapping was done with a very low number of mouse strains, our study was underpowered. This may be another reason for a small number of overlapping loci; a number of loci identified by either method may be false positives. For this reason, we prioritized the loci for further investigation by combining our GWA mapping data with previously established QTLs for innate immune response to LPS and GN pathogens in genetic crosses. Additionally, we assigned higher priority to loci identified by both Plink and EMMA analyses and loci that were associated with multiple cytokine/chemokine strain phenotypes. Although this approach is reasonable for focusing our initial investigation, one limitation is that some of the loci that were not chosen may contain very important and interesting genes that specifically control production of one of the four pro-inflammatory markers.

We next selected genes within the 16 high-priority loci to investigate functionally by utilizing RNA interference in macrophages. We believe that the 38 selected genes are the best candidates for preliminary investigation but acknowledge the fact that there are limitations to our selection. The remaining 34 genes that were not chosen on the basis of the current knowledge of their biological function should also be investigated in the future. Moreover, genes that are not differentially expressed but lie within the boundaries of the remaining 13 loci (~600 genes) should also be prioritized for further examination as they may contain important polymorphisms that do not alter gene expression but affect gene function.

Finally, our investigation of the 38 candidate genes by RNA interference showed that inhibition of 1110058L19Rik, 4933415F23Rik, Fbxo9, and Ipo7 consistently blocked production of IL-6 in mouse macrophages, suggesting a functional role for these

TABLE 2

Differentially expressed genes within 16 *in silico* loci

Chr	Mb	Entrez Gene	Gene symbol	Gene name	Organ (sensitive/resistant fold change in response to LPS)
1	23–28	68002	1110058L19Rik	Hypothetical protein LOC68002 (COG5508, uncharacterized conserved small protein)	Liver (0.6); spleen (0.7)
2	68–70	329416	Nostrin	Nitric oxide synthase trafficker	Liver (1.7)
2	68–70	277395	A130030D10Rik	Hypothetical protein LOC277395 (ZnF_UBR1; putative zinc finger in N-recognin, a recognition component of the N-end rule pathway; domain is involved in recognition of N-end rule substrates in yeast Ubr1p)	Lung (0.7)
2	106.5–109	76894	Mett5d1	Methyltransferase 5 domain containing 1	Liver (1.7)
2	106.5–109	212772	2700007P21Rik	Hypothetical protein LOC212772 (no known domains)	Spleen (1.8)
6	59.5–64	171198	V1rc25	Vomeronasal 1 receptor, C25	Spleen (1.3)
6	59.5–64	27055	Fkbp9	FK506 binding protein 9	Liver (0.7)
7	115–118	16409	Itgam	Integrin alpha M (CR3; CR3A; Cd11b; Ly-40; Mac-1)	Spleen (0.3)
7	82.5–106	18479	Pak1	p21 (CDKN1A)-activated kinase 1	Spleen (0.8)
7	82.5–106	18442	P2ry2	Purinergic receptor P2Y, G-protein coupled 2	Liver (1.5)
7	82.5–106	18332	Olfr33	Olfactory receptor 33	Spleen (1.3)
7	82.5–106	94094	Trim34	Tripartite motif protein 34 (IFP1; RNF21)	Spleen (1.3)
7	82.5–106	20128	Trim30	Tripartite motif protein 30	Spleen (3.1)
7	82.5–106	20597	Smpd1	Sphingomyelin phosphodiesterase 1, acid	Liver (0.8); spleen (0.7)
7	82.5–106	19024	Ppfibp2	Protein tyrosine phosphatase, receptor-type, F	Liver (0.3)
7	82.5–106	258927	Olfr481	Olfactory receptor 481	Spleen (1.3)
7	82.5–106	67150	Rnf141	Ring finger protein 141 (ZFP26; ZNF230; MGC8715)	Lung (0.5)
7	82.5–106	233726	Ipo7	Importin 7 (Ranbp7)	Lung (1.5)
7	82.5–106	21835	Thrsp	Thyroid hormone-responsive protein	Lung (0.2)
7	82.5–106	67800	Dgat2	Diacylglycerol O-acyltransferase 2	Spleen (0.6)
7	82.5–106	11870	Art1	ADP-ribosyltransferase 1	Liver (0.7)
7	82.5–106	76932	Arfip2	ADP-ribosylation factor interacting protein 2	Liver (0.6)
7	82.5–106	14356	Fxc1	Fractured callus expressed transcript 1	Liver (0.8)
7	82.5–106	67967	Pold3	Polymerase (DNA directed), delta 3	Liver (1.7); spleen (2.2)
7	82.5–106	101706	Numa1	Nuclear mitotic apparatus protein 1	Liver (0.7)
7	82.5–106	26451	Rpl27a	Ribosomal protein L27a	Spleen (1.5)
8	21–23.5	64933	Ap3m2	Adaptor-related protein complex 3, mu 2 subunit	Spleen (0.7)
9	78–81.5	14629	Gclc	Glutamate-cysteine ligase, catalytic subunit	Liver (1.8)
9	78–81.5	56542	Ick	Intestinal cell kinase	Spleen (1.3)
9	78–81.5	215351	Senp6	SUMO/sentrin specific protease 6	Lung (1.6)
9	78–81.5	71538	Fbxo9	F-box protein 9 isoform 1	Liver (0.7)
9	78–81.5	214763	E330016A19Rik	Hypothetical protein LOC214763 (Mab-21, Mab-21 protein domain)	Spleen (1.6)
11	56.2–60.2	103836	Zfp692	Zinc finger protein 692	Spleen (0.6)
11	56.2–60.2	94091	Trim11	Tripartite motif protein 11	Liver (2.1)
11	56.2–60.2	216805	Flcn	Folliculin	Liver (1.7)
11	56.2–60.2	14799	Gria1	Glutamate receptor, ionotropic, AMPA1 (alpha 1)	Lung (0.4)
11	56.2–60.2	216767	Mrpl22	Mitochondrial ribosomal protein L22	Spleen (1.3)
11	56.2–60.2	67212	Mrpl55	Mitochondrial ribosomal protein L55	Liver (0.7); spleen (0.8)
13	48–58	27047	Omd	Osteomodulin (osteoadherin, Osad)	Lung (0.3)
13	48–58	23882	Gadd45g	Growth arrest and DNA-damage-inducible 45 gamma	Spleen (1.5)
13	48–58	18030	Nfil3	Nuclear factor, interleukin 3, regulated (IL3bp1)	Spleen (2.7)

(*continued*)

TABLE 2

(Continued)

Chr	Mb	Entrez Gene	Gene symbol	Gene name	Organ (sensitive/resistant fold change in response to LPS)
13	48–58	76577	Ubxd8	Protein expressed in T-cells and eosinophils in atopic dermatatis	Liver (1.5)
13	48–58	66890	Lman2	Lectin, mannose-binding 2	Liver (0.7)
13	48–58	51791	Rgs14	Regulator of G-protein signaling 14	Spleen (0.5)
13	48–58	67399	Pdlim7	PDZ and LIM domain 7	Lung (3.0)
13	48–58	21810	Tgfbi	Transforming growth factor, beta induced	Spleen (0.3)
13	48–58	27261	Dok3	Dok-like protein	Spleen (0.5)
13	48–58	19336	Rab24	RAB24, member RAS oncogene family	Spleen (0.7)
13	48–58	15267	Hist2h2aa1	Histone 2, H2aa1	Liver (1.3)
13	48–58	28126	D13Wsu177e	Hypothetical protein LOC28126 (no known domains)	Liver (0.8)
13	48–58	212483	BC021381	Hypothetical protein LOC212483 (no known domain)	Spleen (0.4)
13	48–58	218271	B4galt7	Xylosylprotein beta 1,4-galactosyltransferase, polypeptide 7	Liver (0.7)
13	48–58	15387	Hnrpk	Heterogeneous nuclear ribonucleoprotein K	Spleen (0.7)
13	48–58	66197	Cks2	CDC28 protein kinase regulatory subunit 2	Liver (0.4)
13	48–58	18081	Ninj1	Ninjurin 1	Liver (0.7)
14	27–30	23955	Nek4	NIMA (never in mitosis gene a)-related kinase 4	Liver (0.6)
14	27–30	239027	Arhgap22	Rho GTPase activating protein 22	Spleen (0.6)
14	27–30	67011	Mettl6	Methyltransferase like 6	Spleen (1.3)
14	27–30	76485	Glt8d1	Glycosyltransferase 8 domain containing 1	Liver (0.6)
14	27–30	56794	Hacl1	2-hydroxyphytanoyl-CoA lyase	Liver (0.3)
14	27–30	53600	Timm23	Translocase of inner mitochondrial membrane 23	Spleen (1.6)
15	31.5–33	223455	March6	Membrane-associated ring finger (C3HC4) 6	Liver (1.3)

four genes in innate immune response to LPS. However, genes whose inhibition by RNAi did not affect cytokine production in J774A.1 macrophages should not be disregarded as potentially important in innate immunity. There are several limitations to the RNAi assay that we utilized in this study. First, the assay was performed in a cultured macrophage cell line and not *in vivo*. Second, some of our candidate genes may regulate innate immunity through mechanisms that do not affect cytokine production and their function may be revealed in assays that measure other phenotypes such as production of superoxide or nitric oxide, phagocytosis, apoptosis, etc. Finally, RNA interference is not always effective in silencing target genes due to a number of factors, including the chosen siRNA sequence and the structure of the siRNA.

The gene 1110058L19Rik is located in locus 1 (Table 1), which is associated with IL-1β and IL-6 phenotypes by Plink mapping as well as the KC phenotype by EMMA mapping, and also overlaps with the Ses1.1 QTL controlling bacterial load in the spleen in response to iv *Salmonella enteritidis* (Caron *et al.* 2002, 2005). In addition, 1110058L19Rik is downregulated in the liver and the spleen of mice sensitive to systemic LPS challenge (Table 2) and its inhibition by RNA interference significantly and consistently decreases production of IL-6 in macrophages (Figure 4). 1110058L19Rik is a gene of unknown function with an uncharacterized conserved small protein domain. Since there are no published studies on this gene, it is difficult to speculate how it may be involved in innate immunity; however, its novelty also makes it an attractive candidate for further study.

Similarly, 4933415F23Rik is also located in locus 1 and also regulates IL-6 production in LPS-stimulated macrophages; however, it is not differentially expressed in response to systemic LPS. The gene 4933415F23Rik is also of unknown function, and has not been studied previously. It contains a protein kinase C (PKC)-activated protein phosphatase-1 inhibitor conserved domain that is involved in modulation of the contractility of vascular smooth muscle, but nothing else is known about this gene.

Fbxo9 is located in locus 9, which was mapped to the IL-1β and IL-6 phenotypes by the Plink method and overlaps with the Ses2 locus that controls bacterial load in the spleen in response to iv *S. enteritidis* (Caron *et al.* 2002, 2005). Moreover, Fbxo9 is significantly downregulated in the liver of LPS-sensitive strains of mice, and it has a phenotype in our RNA-interference assay in macrophages. The function of Fbxo9 is unknown, but it is possible that it may be involved in polyubiquitination of IκB or another important signaling molecule in the TLR4 pathway or another pathway that is activated in response to LPS (Fong and Sun 2002).

Finally, importin 7 (Ipo7) is in locus 7, which is associated with IL-6 and TNFα phenotypes by Plink mapping as well as the KC phenotype by EMMA mapping. Ipo7 is significantly induced in the lung of

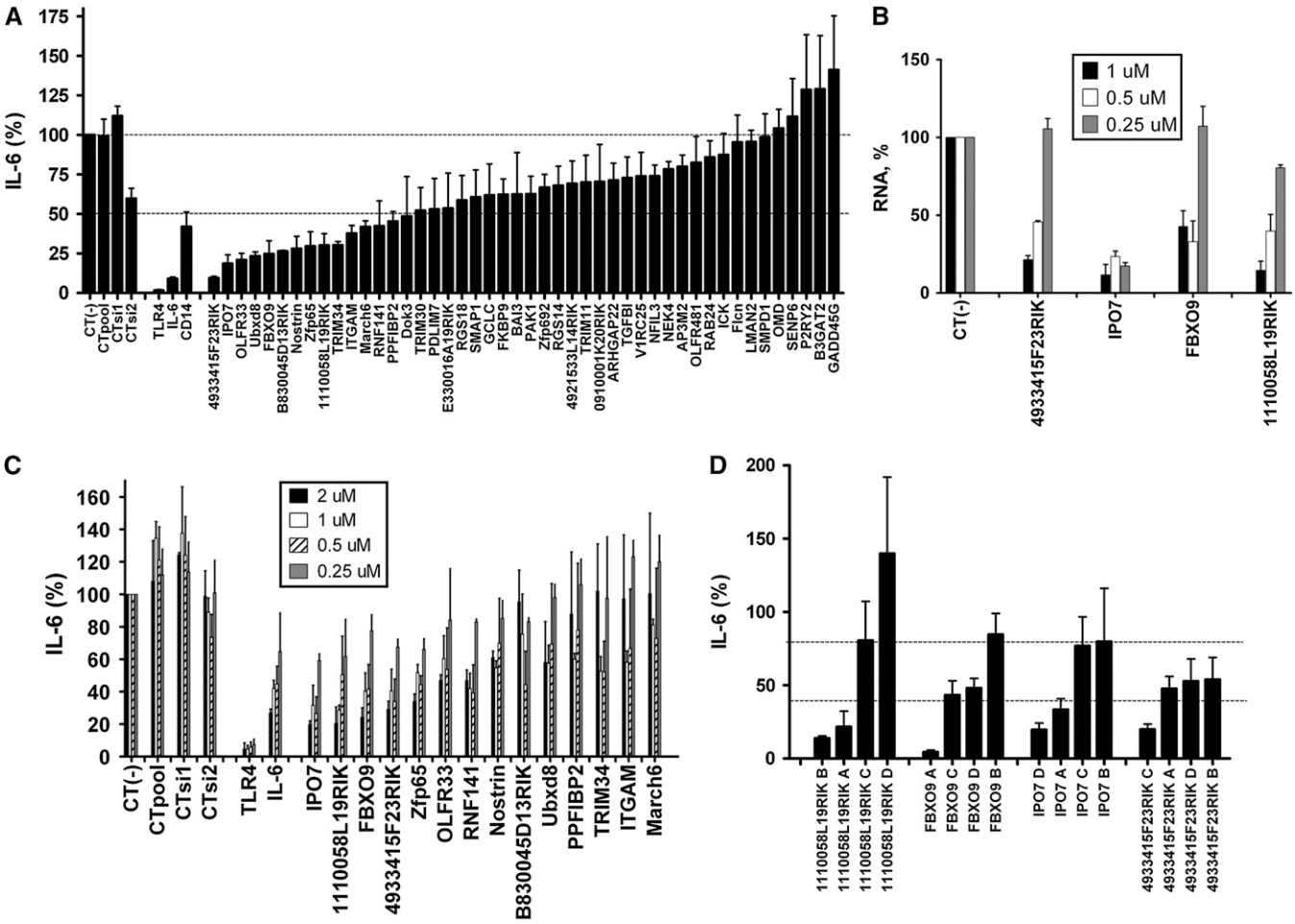

FIGURE 4.—An RNA interference assay in cultured macrophages identifies four genes that regulate cytokine production. (A) The effect of siRNA-mediated gene inhibition in the J77A4.1 macrophage cell line on IL-6 production in response to LPS stimulation. A pool of four siRNA duplexes was transfected for each gene. Shown are the results for four negative controls (all data are normalized to the first negative control), three positive controls, and 34 candidates from our analysis. (B) Inhibition of IL-6 production by J774A.1 macrophages in response to LPS by different concentrations of siRNA pools. (C) Gene expression knockdown by different concentrations of siRNA pools monitored using qPCR. The extent of gene inhibition roughly correlates with the phenotype in panel B. (D) Four genes that consistently affected cytokine production in the initial pooled siRNA screen (panel A) and siRNA titrations (panel B) were retested using each of the individual siRNAs in the pool. All four siRNAs were transfected individually, the cells were stimulated with LPS, and the supernatant was assayed for IL-6 production by ELISA. In all panels, means of three independent measurements are plotted with error bars representing standard deviations.

sensitive strains of mice in response to systemic LPS, and its inhibition by RNA interference inhibits the production of IL-6 in macrophages. Ipo7 was recently shown to be one of the import receptors for the transcription factor c-Jun, a component of the transcriptional complex AP-1 (WALDMANN *et al.* 2007). It is feasible that the role of importin 7 in nuclear import of c-Jun explains its involvement in the murine response to LPS as it is well established that AP-1 is activated in response to LPS via MAP kinases (LIEW *et al.* 2005). However, importin 7 also controls transport of many other molecules and could therefore have a role in LPS signaling through other presently unknown mechanisms.

In summary, our whole genome association analysis of inbred murine strain phenotypes combined with previously established QTL, gene expression, and RNA interference data identified four novel genes that regulate the host response to systemic LPS. We believe that the function of these genes in innate immunity should be further investigated using targeted mutations in mice and other approaches. However, as discussed above, there are several limitations to the way we used to prioritize and functionally study candidates, and it is likely that other genes identified by whole genome association mapping could also be important targets of LPS signaling *in vivo*. Additional genetic and genomic studies, namely, whole genome association mapping of phenotypes other than pro-inflammatory cytokines and chemokines, such as survival, other genetic crosses in mice, and *in vivo* RNA interference, will aid in identification of other important candidates that mediate the host response to LPS.

This study was funded by the Department of Veterans Affairs (merit review), the National Institute of Environmental Health Sciences (ES11375 and ES011961), and the Intramural Research Program of the National Institutes of Health, National Institute of the Environmental Health Sciences, and National Heart, Lung, and Blood Institute.

LITERATURE CITED

Akira, S., and K. Takeda, 2004 Toll-like receptor signalling. Nat. Rev. Immunol. **4:** 499–511.

Alper, S., R. Laws, B. Lackford, W. A. Boyd, P. Dunlap *et al.*, 2008 Identification of innate immunity genes and pathways using a comparative genomics approach. Proc. Natl. Acad. Sci. USA **105:** 7016–7021.

Baron, R. M., M. J. Baron and M. A. Perrella, 2006 Pathobiology of sepsis: Are we still asking the same questions? Am. J. Respir. Cell. Mol. Biol. **34:** 129–134.

Buras, J. A., B. Holzmann and M. Sitkovsky, 2005 Animal models of sepsis: setting the stage. Nat. Rev. Drug Discov. **4:** 854–865.

Caron, J., J. C. Loredo-Osti, L. Laroche, E. Skamene, K. Morgan *et al.*, 2002 Identification of genetic loci controlling bacterial clearance in experimental Salmonella enteritidis infection: an unexpected role of Nramp1 (Slc11a1) in the persistence of infection in mice. Genes Immun. **3:** 196–204.

Caron, J., J. C. Loredo-Osti, K. Morgan and D. Malo, 2005 Mapping of interactions and mouse congenic strains identified novel epistatic QTL controlling the persistence of Salmonella enteritidis in mice. Genes Immun. **6:** 500–508.

Cook, D. N., D. S. Pisetsky and D. A. Schwartz, 2004a Toll-like receptors in the pathogenesis of human disease. Nat. Immunol. **5:** 975–979.

Cook, D. N., S. Wang, Y. Wang, G. P. Howles, G. S. Whitehead *et al.*, 2004b Genetic regulation of endotoxin-induced airway disease. Genomics **83:** 961–969.

De Maio, A., M. L. Mooney, L. E. Matesic, C. N. Paidas and R. H. Reeves, 1998 Genetic component in the inflammatory response induced by bacterial lipopolysaccharide. Shock **10:** 319–323.

Fong, A., and S. C. Sun, 2002 Genetic evidence for the essential role of beta-transducin repeat-containing protein in the inducible processing of NF-kappa B2/p100. J. Biol. Chem. **277:** 22111–22114.

Frazer, K. A., E. Eskin, H. M. Kang, M. A. Bogue, D. A. Hinds *et al.*, 2007 A sequence-based variation map of 8.27 million SNPs in inbred mouse strains. Nature **448:** 1050–1053.

Fulton, W. B., R. H. Reeves, M. Takeya and A. De Maio, 2006 A quantitative trait loci analysis to map genes involved in lipopolysaccharide-induced inflammatory response: identification of macrophage scavenger receptor 1 as a candidate gene. J. Immunol. **176:** 3767–3773.

Garantziotis, S., J. W. Hollingsworth, A. K. Zaas and D. A. Schwartz, 2008 The effect of toll-like receptors and toll-like receptor genetics in human disease. Annu. Rev. Med. **59:** 343–359.

Grupe, A., S. Germer, J. Usuka, D. Aud, J. K. Belknap *et al.*, 2001 In silico mapping of complex disease-related traits in mice. Science **292:** 1915–1918.

Kang, H. M., N. A. Zaitlen, C. M. Wade, A. Kirby, D. Heckerman *et al.*, 2008 Efficient control of population structure in model organism association mapping. Genetics **178:** 1709–1723.

Liew, F. Y., D. Xu, E. K. Brint and L. A. O'Neill, 2005 Negative regulation of toll-like receptor-mediated immune responses. Nat. Rev. Immunol. **5:** 446–458.

Liu, P., Y. Wang, H. Vikis, A. Maciag, D. Wang *et al.*, 2006 Candidate lung tumor susceptibility genes identified through whole-genome association analyses in inbred mice. Nat. Genet. **38:** 888–895.

Lorenz, E., M. Jones, C. Wohlford-Lenane, N. Meyer, K. L. Frees *et al.*, 2001 Genes other than TLR4 are involved in the response to inhaled LPS. Am. J. Physiol. Lung Cell Mol. Physiol. **281:** L1106–L1114.

Matesic, L. E., A. De Maio and R. H. Reeves, 1999 Mapping lipopolysaccharide response loci in mice using recombinant inbred and congenic strains. Genomics **62:** 34–41.

Matesic, L. E., E. L. Niemitz, A. De Maio and R. H. Reeves, 2000 Quantitative trait loci modulate neutrophil infiltration in the liver during LPS-induced inflammation. FASEB J. **14:** 2247–2254.

McClurg, P., J. Janes, C. Wu, D. L. Delano, J. R. Walker *et al.*, 2007 Genomewide association analysis in diverse inbred mice: power and population structure. Genetics **176:** 675–683.

Morton, D. B., and P. H. Griffiths, 1985 Guidelines on the recognition of pain, distress and discomfort in experimental animals and an hypothesis for assessment. Vet. Rec. **116:** 431–436.

Papathanassoglou, E. D., M. D. Giannakopoulou and E. Bozas, 2006 Genomic variations and susceptibility to sepsis. AACN Adv. Crit. Care **17:** 394–422.

Pletcher, M. T., P. McClurg, S. Batalov, A. I. Su, S. W. Barnes *et al.*, 2004 Use of a dense single nucleotide polymorphism map for in silico mapping in the mouse. PLoS Biol. **2:** e393.

Purcell, S., B. Neale, K. Todd-Brown, L. Thomas, M. A. Ferreira *et al.*, 2007 PLINK: a tool set for whole-genome association and population-based linkage analyses. Am. J. Hum. Genet. **81:** 559–575.

Sebastiani, G., L. Olien, S. Gauthier, E. Skamene, K. Morgan *et al.*, 1998 Mapping of genetic modulators of natural resistance to infection with Salmonella typhimurium in wild-derived mice. Genomics **47:** 180–186.

Svoboda, P., 2007 Off-targeting and other non-specific effects of RNAi experiments in mammalian cells. Curr. Opin. Mol. Ther. **9:** 248–257.

Wade, C. M., and M. J. Daly, 2005 Genetic variation in laboratory mice. Nat. Genet. **37:** 1175–1180.

Waldmann, I., S. Walde and R. H. Kehlenbach, 2007 Nuclear import of c-Jun is mediated by multiple transport receptors. J. Biol. Chem. **282:** 27685–27692.

Communicating editor: G. Gibson

GENETICS

Supporting Information
http://www.genetics.org/cgi/content/full/genetics.109.107540/DC1

Identification of Novel Genes That Mediate Innate Immunity Using Inbred Mice

Ivana V. Yang, Claire M. Wade, Hyun Min Kang, Scott Alper, Holly Rutledge, Brad Lackford, Eleazar Eskin, Mark J. Daly and David A. Schwartz

DOI: 10.1534/genetics.109.107540

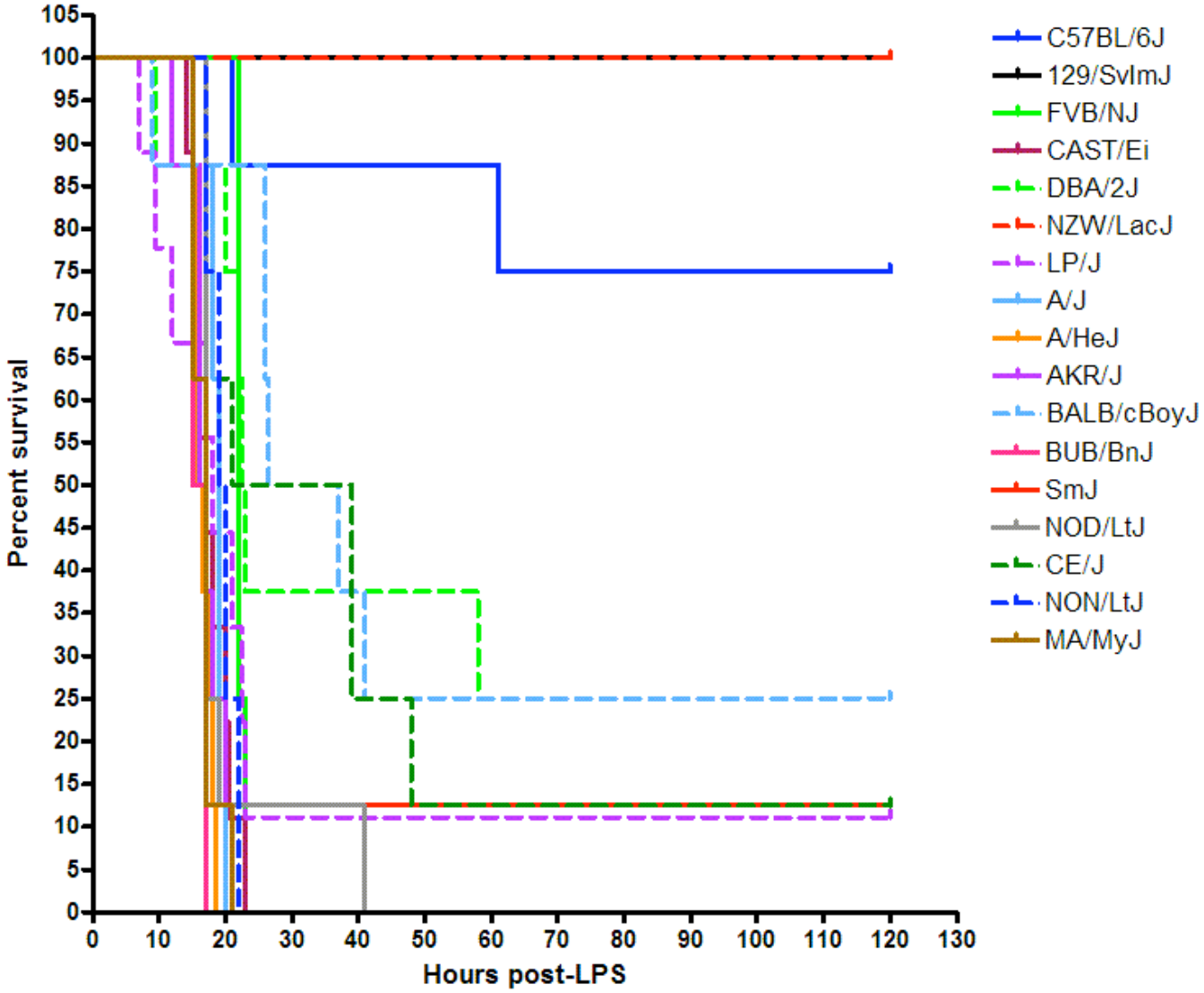

FIGURE S1.—Kaplan-Meier survival curves for 16 murine strains challenged with LPS intraperitoneally (N=16). Two strains (129/SvIm and NZW/LacJ) are completely unresponsive to systemic administration of LPS (100% survival 5 days post-LPS). In addition, 75% of C57BL/6J mice survive for 5 days and are also considered resistant to LPS. The remaining 13 strains have <25% survival and are therefore sensitive to LPS challenge.

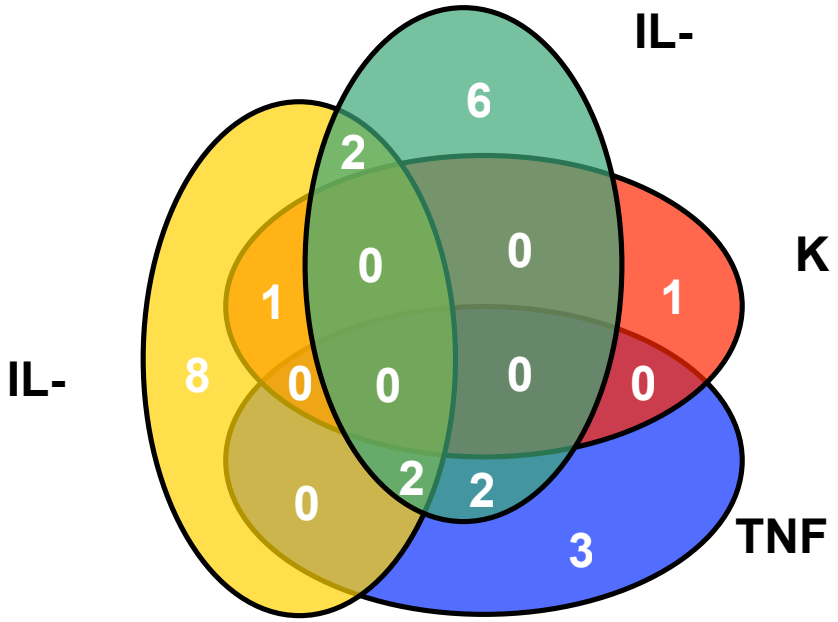

A

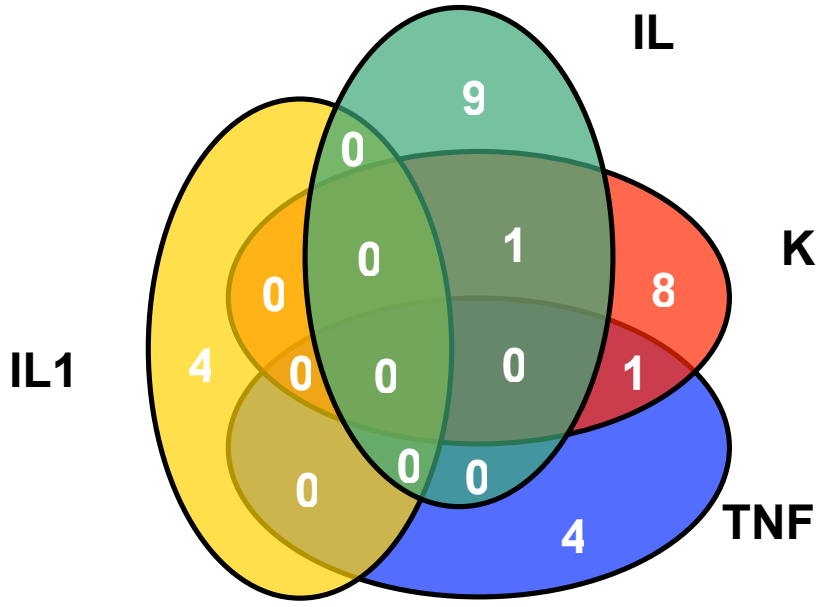

B

Figure S2.—(A) Venn diagram depicting loci that are significantly ($p < 1x10^{-5}$) associated with TNFα, IL-1β, IL-6, and KC phenotypes identified by whole genome association mapping using Plink. (B) Venn diagram depicting loci that are significantly ($p < 0.001$) associated with TNFα, IL-1β, IL-6, and KC phenotypes determined by whole genome association mapping using EMMA.

TABLE S1

Top statistically significant loci identified by the whole genome association mapping using Plink software

Trait	Chr	SNP marker location, Mb	p value
IL1β	1	1-26427831	3.90E-10
IL1β	4	4-118929601	3.90E-10
IL1β	6	6-55773821, 6-56347198, 6-56678621	3.90E-10
IL1β	7	7-9595330,	3.90E-10
IL1β	7	7-116601809	3.90E-10
IL1β	8	8-11407267, 8-11545200	3.90E-10
IL1β	8	8-15437088, 8-15887993	3.90E-10
IL1β	9	9-71978202	3.90E-10
IL1β	9	9-80149240	3.90E-10
IL1β	14	14-28372705	3.90E-10
IL1β	14	14-91942359, 14-92310781	3.90E-10
IL1β	15	15-32541454	3.90E-10
IL1β	15	15-73971286, 15-74703498	3.90E-10
IL6	1	1-26445071, 1-26459079, 1-26902686	4.90E-07
IL6	3	3-129840133	4.90E-07
IL6	4	4-66474304	4.90E-07
IL6	5	5-79316768, 5-79549852, 5-80265545	4.90E-07
IL6	6	6-61560974	4.40E-08
IL6	7	7-8853602, 7-9333316	4.40E-08
IL6	7	7-116916407	4.90E-07
IL6	9	9-80661899	4.40E-08
IL6	9	9-91743675	4.90E-07
IL6	14	14-28800101	4.90E-07
IL6	15	15-32504050, 15-32506173	4.9E-07, 4.4E-08
IL6	16	16-74996799	4.40E-08
KC	1	1-42359021	1.20E-07
KC	1	1-145683060	1.20E-07
KC	2	2-69438537	1.20E-07
KC	2	2-80841547, 2-80883004, 2-81138233, 2-81560669, 2-81615533, 2-81617733, 2-81628234, 2-81658448, 2-81659050, 2-81678285, 2-81704287, 2-81718343, 2-81789194, 2-82079297, 2-82079512, 2-82084458, 2-82117829, 2-82122611, 2-82126777, 2-82143108, 2-82143635	1.20E-07
KC	8	8-22416276, 8-22536836	1.20E-07
KC	9	9-102485822, 9-102486025, 9-102795058, 9-102820141	1.20E-07
KC	10	10-12531822	1.20E-07
KC	11	11-33472763	1.20E-07
KC	13	13-15857142	1.20E-07

KC	13	13-17935945, 13-17939094, 13-18007167, 13-18013901, 13-18015558, 13-18034732, 13-18078449, 13-18088391,	1.20E-07
KC	13	13-18838101, 13-18841477	1.20E-07
KC	13	13-19997527, 13-20357183, 13-20362181, 13-20762951	1.20E-07
KC	13	13-44918729, 13-44927393	1.20E-07
KC	14	14-92145464	1.20E-07
KC	17	17-6618636	1.20E-07
TNFα	1	1-156166139, 1-156202467, 1-156260700	6.3E-06, 9.1E-06
TNFα	5	5-139522305, 5-145235709	7.4E-06, 9.1E-06
TNFα	6	6-61560974	5.20E-06
TNFα	7	7-8853602, 7-9333316	5.20E-06
TNFα	9	9-79331943, 9-80661899	5.2E-06, 9.1E-06
TNFα	11	11-94538851	4.70E-06
TNFα	15	15-32506173	5.20E-06

TABLE S2

Top statistically significant loci identified by the whole genome association mapping using the EMMA method

Trait	Chr	SNP marker location, Mb	p value
IL1β	2	107315924, 107357384, 107398624, 107412136, 107959779, 108073860, 108185629,	5.40E-03
IL1β	2	158272211	5.40E-03
IL1β	3	47660671, 47785264, 47836055, 47859157, 47919658, 48030639, 48159888, 49874886, 49875179, 49937044, 50010267, 50033628, 50847321, 50873461, 50956019, 50976395, 51029209, 51056033, 51095526	5.40E-03
IL1β	5	141174147	5.40E-03
IL6	4	43762232	8.00E-04
IL6	7	47687584, 47876910	8.00E-04
IL6	8	14516743, 14916293, 14916239, 18379632	8E-4, 1.2E-3, 1.3E-3, 1.5E-3, 1.4E-3
IL6	8	22106945, 22224999, 22185337, 22262697, 22277352, 22115030,	8E-4, 1.2E-3, 1.3E-3, 1.5E-3, 1.4E-3
IL6	10	62958029, 63177650	1.40E-03
IL6	11	59250160	8.00E-04
IL6	12	23700515	1.20E-03
IL6	13	3367757,	1.40E-03
IL6	13	5173293, 5273676, 5461529, 5675544,	1.40E-03
IL6	14	43772111	1.20E-03
KC	1	24076131, 24330584, 24967418, 24967436, 26414682	5.6E-3, 6.8E-3
KC	3	66022799	5.80E-03
KC	4	550141012, 51252642,	5.8E-3, 6.9E-3
KC	4	67306119	5.8E-3, 6.9E-3
KC	5	80712378, 81426649	6.80E-03
KC	6	62063800, 61240554	6.9E-3, 7.1E-3
KC	7	15561520	6.80E-03
KC	7	125532752,	5.2E-3,
KC	11	57287378	5.60E-03
KC	14	28903045	6.10E-03
TNFα	1	14672597	6.40E-03
TNFα	4	53927543, 53804390, 53769939	1.7E-3, 6.4E-3
TNFα	10	84840338	4.40E-03
TNFα	15	36483892, 3646795, 36545156	6.90E-03
TNFα	18	58969828	4.90E-03

TABLE S3

Known genes in the 16 high-priority *in silico* loci

Locus #	Chr	Locus Boundaries, Mb	Known Genes
1	1	23-28	Bai3, 4933415F23Rik, B3gat2, Smap1, 1110058L19Rik, 4921533L14Rik, Col9a1, Col19a1, Lmbrd1
2	1	145.5-147	Rgs18, B830045N13Rik
3	2	68-70	B3galt1, Stk39, 4933409G03Rik, 4932414N04Rik, Lass6, Nostrin, Spbc25, G6pc2, Abcb11, Dhrs9, Bbs5, Fastkd1, Phospho2, Klhl23, Ssb, A130030D10Rik
4	2	80.5-82.5	none
5	2	106.5-109	C130023O10Rik, 2700007P21Rik, Fshb, Kcna4, Mett5d1
6	5	78-82	none
7	6	59.5-64	A530053G22Rik, Snca, Pde1c, Lsm5, Kbtbd2, Fkbp9, Nt5c3, V1rc21, V1rc19, V1rc20, V1rc32, V1rc1, V1rc30, V1rc3, V1rc5, V1rc7, V1rc6, V1rc29, V1rc16, V1rc26, V1rc27, Ppm1k, Pigy, Lancl2, AW146242, V1rc28, V1rc23, V1rc24, V1rc1865, V1rc17, V1rc33, V1rc25, V1rc2, V1rc22, Abcg2, Herc3, Nap1l5, D430015B01Rik, Gprin3
8	7	82.5-106	Odz4, Nars2, Alg8, Ndufc2, Thrsp, Ints4, 1810020D17Rik, 1810020D17Rik, Clns1a, Aqp11, Pak1, Gdpd4, Myo7a, Capn5, Phca, A630091E08Rik, 2210018M11Rik, Prkrir, Wnt11, Uvrag, Dgat2, Mogat2, Mtap6, Serpinh1, Gdpd5, Rps3, Arrb1, Slco2b1, Olfr52065, Neu3, Spcs2, D930018N13, Chrdl2, Pold3, 2610209A20Rik, Kcne3, Pgm2l1, P4ha3, Ppme1, Ucp3, Ucp2, Dnajb13, Chchd8, D630004N19Rik, Mrpl48, Rab6, Plekhb1, Tnfrsf19l, P2ry6, P2ry2, Fchsd2, Stard10, Centd2, Art2a, Clpb, Phox2a, Inppl1, Folr2, Folr1, 3200002M19Rik, 2400001E08Rik, Art1, Art5, Rnf121, Il18bp, Numa1, Trpc2, Frag1, Rhog, Stim1, Rrm1, Olfr544, Olfr545, Olfr547, Olfr549, Trim21, Olfr550, Olfr551, Olfr552, Olfr553, Olfr554, Olfr555, Olfr565, Trim68, Olfr557, Olfr558, Olfr33, Olfr559, Olfr78, Olfr560, Olfr561, Olfr564, Olfr569, Olfr570, Olfr571, Olfr572, Olfr574, Olfr575, Olfr576, Olfr577, Olfr578, Olfr583, Olfr584, Olfr585, Olfr586, Olfr589, Olfr592, Olfr593, Olfr594, Dub2a, Olfr599, Olfr600, Olfr601, Olfr604, Dub2, Olfr606, Olfr608, Olfr609, Olfr610, Olfr611, Olfr614, Olfr615, Olfr616, Olfr617, Olfr618, Olfr619, Olfr620, Olfr622, Olfr623, Olfr630, Olfr628, Olfr629, Olfr68, Olfr69, Olfr67, Hbb-b2, Hbb-b1, Hbb-bh1, Hbb-y, Olfr631,Olfr632,Olfr66,Olfr65,Olfr64,Olfr633, Olfr635, Olfr638, Olfr639, Olfr640, Olfr641, Olfr642, Olfr643, Olfr644, Olfr645, Olfr646, Ubqln3, Ubqlnl, E030002O03Rik, Olfr648, Olfr649, Trim34, Trim12, 9230105E10Rik, A530023O14Rik, AI451617, Olfr651, Olfr652, Olfr653, Olfr654, Olfr655, Olfr656, Olfr657, Olfr658, Olfr659, Olfr661, Dub1a, Dub1, Olfr665, Olfr666, Olfr667, Olfr668, Olfr669, Olfr672,Olfr672,Olfr676, Olfr677, Olfr678, Olfr679, Olfr681, Olfr683, Olfr684, Olfr686, Olfr689, Olfr690, Olfr691, Olfr692, 4632419K20Rik, Cckbr, Prkcdbp, Smpd165, Hpxn, Trim3, Arfip2, Fxc1, 1500003O22Rik, Ilk, Taf10, Tpp1,

			Mrpl17, Gvin1, Olfr693, Olfr694, Olfr695, Olfr697, Olfr698, Olfr700, Olfr701, Olfr703, Olfr705, Olfr706, Olfr710, Olfr6, Olfr711, Olfr2, Olfr713, Olfr714, Olfr17O, lfr715, Olfr716, Syt9, Olfml1, Ppfibp2, Cyb5r2, Ovch2, Olfr469, Olfr473, Olfr474, Olfr476, Olfr477, Olfr481, Olfr478 ,Olfr480, Olfr482, Olfr483, Olfr484, Olfr486, Olfr488, Olfr490, Olfr491, Olfr492, Olfr493, Olfr494, Olfr495, Olfr497, Olfr498, Olfr502, Olfr507, Olfr508, Olfr509, Olfr510, Olfr512, Olfr513, Olfr514, Olfr516, Olfr518, Nlrp10, Eif3s5, Tub, Ric3, Lmo1, Trim66, D930014E17Rik, Ascl3, Tmem9b, Nrip3, Scube2, Phxr5, Rab6ip1, Tmem41b, Ipo7, Zfp143, Wee1, Swap70, Adm, Ampd3, Rnf141, Xlkd1, Ctr9, Eif4g2, Galntl4, Usp47, Dkk3, Mical2, Parva, Tead1, Pik3c2a, 4632411J06Rik, Arntl, A630005I04Rik, Btbd10, Pth, Mlstd2, Spon1, Rras2, Copb1, Psma165, Cyp2r1, Calca, Insc, Sox6, 1110004F10Rik, Plekha7, Rps13, Nucb2, Xylt1, Arl6ip, 14930583K01Rik, Syt17, Coq7, Tmc7, Tmc5, Mir16
9	7	115-118	Armcx3, Itgam, Itgax, Cox6a2, Armc5, Tgfb1i1, Slc5a2, BC017158, Rgs10, Tial1, Bag3, Inpp5f, 1110007A13Rik, Brwd2, Fgfr2, Rfwd3, Ate1, Phkg2, Rnf40, 1700120K04Rik, Zfp629, Bcl7c, Ctf1, Ctf2, Fbxl19, Tmem142c, Setd1a, Hsd3b7, Stx1b2, Stx4a, Zfp668, Vkorc1, Bckdk, Myst1, Prss8, Fus, B230325K18Rik, Pycard
10	8	21-23.5	Thsd1, Slc25a15, Mrps31, Slc20a2, Vdac3, Dkk4, PolbIkbkb, Plat, Ap3m2, 1700041G16Rik, Ank1, Agpat6, Gins4, Golga7, Sfrp1, Zmat4, A730045E13Rik, 1810011O10Rik, Indol1, Adam18, Adam3
11	9	78-81.5	Gclc, Elovl5, Gcm1, Fbxo9, Ick, Gsta4, Dppa5, Omt2b, Gsta2, Gsta1, 2410146L05Rik, E330016A19Rik, Mto1, Slc17a5, Cd109 Col12a1, Cox7a2, Tmem30a, Senp6, Impg1
12	11	56.2-60.2	Gria1, 1810073G14Rik, Mfap3, Galnt10, Hand1, Cnot8, Gemin5, Mrpl22, Igtp, Iigp2, Zfp692, Zfp672, Sh3bp5, l1810065E05Rik, 4930504O13Rik, Olfr30, Olfr330, Olfr328, Olfr325, 2210407C18Rik, Olfr323, Olfr320, Olfr319, Olfr318, Olfr315, Olfr313, Olfr311, 2810021J22Rik, Zfp39 Butr1, Hist3h2ba, Hist3h2bb, Trim17, Trim11, A230051G13Rik, 4930543L23Rik, Gja12, Guk1, Mrpl55, 2310033P09Rik, Arf1, Wnt3a, Wnt9a, 1110031B06Rik, Jmjd4, Zfp496, Nlrp3, Olfr223, AA536749, Flcn, Cops3, Nt5m, Med9, Rasd1, Pemt, 4930412M03Rik Rai1 Srebf1, Tom1l2, Lrrc48 Atpaf2, 4933439F18Rik, Drg2, Myo15, Alkbh5
13	13	48-58	AW456874, Barx1, Phf2, Ninj1, 1110007C09Rik, Susd3, Fgd3, Bicd2, Ippk, Cenpp, Aspn, Omd, Ogn, Iars, Fbxw17, Spin1, 4930519N16Rik, Hist2h2aa1, Edg3, Shc3, Cks2, Sema4d, Gadd45g, Syk, Auh, Nfil3, Ror2, Sptlc1, Msx2, Drd1a, Sfxn1, Hrh2, Cplx2, Thoc3, 4732471D19Rik, Arl10, D13Wsu177e, Higd2a, Cltb Ubxd8, Rnf44, Gprin1, Sncb, Tspan17, Unc5a, Uimc1, Rpl29, Zfp346, Fgfr4, Nsd1, Rab24, 2610524G07Rik Mxd3, Lman2, Rgs14, Slc34a1, Pfn3, F12, Gprk6, Dbn1, Pdlim7, Dok3, Ddx41, BC021381, Tmed9, B4galt7, Caml, B230219D22Rik, 2310047H23Rik, 4930451E10Rik, Catsper3, Pitx1, H2afy, BC027057, Neurog1, Cxcl14, AU042651Il9, Fbxl21, Lect2, Tgfbi, Smad5, Trpc7, Spock1, 5133401N09Rik, Ubqln1, Gkap1, Kif27, Hnrpk, Rmi1, Slc28a3, Ntrk2

14	14	27-30	Nek4, Spcs1, Glt8d1, Gnl3, Stab1, Nisch, Tnnc1, Phf7, Bap1, Capn7, Sh3bp5, Mettl6, Eaf1, Hacl1, Btd, D830044D21Rik, Dph3, Oxnad1, Msmb, Ncoa4, Timm23, Parg, Chat, Slc18a, 39430077A04Rik, Prrxl1, E130203B14Rik, Lrrc18, Arhgap22, Mapk8, Ptpn20, Gdf10, Gdf2, Rbp3
15	14	91.3-93	Dis3, Klf5, Klf12
16	15	31.5-33	Tas2r119, Sema5a, Sdc2, Ropn1l, March6, Cmbl, Cct5